How Do Sinking Phytoplankton Species Manage to Persist?

Jef Huisman,[1,*] **Manuel Arrayás,**[2,3,†] **Ute Ebert,**[2,‡] **and Ben Sommeijer**[2,§]

1. Aquatic Microbiology, Institute for Biodiversity and Ecosystem Dynamics, University of Amsterdam, Nieuwe Achtergracht 127, 1018 WS Amsterdam, The Netherlands;
2. Center for Mathematics and Computer Science (CWI), P.O. Box 94079, 1090 GB Amsterdam, The Netherlands;
3. Lorentz Institute, University of Leiden, P.O. Box 9506, 2300 RA Leiden, The Netherlands

ABSTRACT: Phytoplankton require light for photosynthesis. Yet, most phytoplankton species are heavier than water and therefore sink. How can these sinking species persist? Somehow, the answer should lie in the turbulent motion that redisperses sinking phytoplankton over the vertical water column. Here, we show, using a reaction-advection-diffusion equation of light-limited phytoplankton, that there is a turbulence window sustaining sinking phytoplankton species in deep waters. If turbulent diffusion is too high, phytoplankton are mixed to great depths, and the depth-averaged light conditions are too low to allow net positive population growth. Conversely, if turbulent diffusion is too low, sinking phytoplankton populations end up at the ocean floor and succumb in the dark. At intermediate levels of turbulent diffusion, however, phytoplankton populations can outgrow both mixing rates and sinking rates. In this way, the reproducing population as a whole can maintain a position in the well-lit zone near the top of the water column, even if all individuals within the population have a tendency to sink. This theory unites earlier classic results by Sverdrup and Riley as well as our own recent findings and provides a new conceptual framework for the understanding of phytoplankton dynamics under the influence of mixing processes.

Keywords: critical depth, export production, light limitation, phytoplankton blooms, reaction-diffusion equation, turbulence.

* E-mail: jef.huisman@science.uva.nl.

† Present address: Escuela Superior de Ciencias y Tecnologia, Universidad Rey Juan Carlos, Calle Tulipan s/n, 28933 Mostoles, Madrid, Spain; e-mail: m.arrayas@escet.urjc.es.

‡ E-mail: Ute.Ebert@cwi.nl.

§ E-mail: B.P.Sommeijer@cwi.nl.

Phytoplankton require light for living. Hence, in order to proliferate, phytoplankton populations should stay in the well-illuminated upper regions of the water column, the so-called euphotic zone. However, many, if not most, phytoplankton species have a higher density than water. They sink (Hutchinson 1967; Smayda 1970; Reynolds 1984). Yet, sinking phytoplankton species have formed a successful part of the phytoplankton community in lakes and oceans for millions of years. How do populations of sinking phototrophic organisms manage to persist? Which environmental factors allow survival of sinking phytoplankton?

Previous studies provided partial answers to these questions. In a classic article, Riley et al. (1949) derived a relation between sinking velocity and water-column turbulence that would just allow the persistence of a sinking phytoplankton population. Although Riley et al. (1949) focused on the interplay between sinking velocity and turbulent diffusion, their mathematical analysis neglected the light dependence of phytoplankton growth. Later, Shigesada and Okubo (1981) reproduced the result of Riley et al. in a model in which they incorporated light-dependent growth rates but neglected light absorption by the water column. In another classic article, Sverdrup (1953) derived the existence of a "critical depth" of the mixed layer beyond which phytoplankton growth would be impossible. Sverdrup's critical-depth theory gained much impetus in modern oceanography and aquatic ecology (e.g., Platt et al. 1991; Kirk 1994; Mann and Lazier 1996; Lucas et al. 1998; Huisman 1999). However, though Sverdrup considered light-dependent growth rates as well as light absorption by the water column, he assumed a uniform phytoplankton depth profile, thereby neglecting implications of both turbulent diffusion and sinking. Recently, Huisman et al. (1999*b*, 1999*c*) derived the existence of a "critical turbulence" that just allows phytoplankton bloom development. Huisman et al. focused on the interplay between turbulent diffusion and light-dependent growth rates but treated sinking phytoplankton only superficially. How do these different concepts fit together? Is there any consistency or overlap between these theories? It feels as if we have different pieces of a complicated puzzle at hand, while the coherent picture is still lacking.

The issue is not without relevance. Sinking phytoplank-

ton play a key role in several biogeochemical cycles because they withdraw nutrients from the upper water column and deposit these nutrients at the bottom sediment or in deep water layers. In particular, sinking phytoplankton have a major impact on the global carbon cycle by exporting photosynthetic carbon from the surface into the deep ocean interior (Falkowski et al. 1998; Arrigo et al. 1999; DiTullio et al. 2000). A better understanding of the population dynamics of sinking phytoplankton species may thus contribute to a better understanding of the biogeochemical cycling of elements in aquatic ecosystems.

In this article, we develop a population-dynamic theory of sinking phytoplankton. The theory is based on a reaction-advection-diffusion equation that considers the balance between light-dependent growth rates, mortality rates, sinking rates, and turbulent-diffusion rates. This reaction-advection-diffusion equation lies at the heart of a wide variety of detailed simulation models in oceanography and ecosystems research (e.g., Jamart et al. 1977; Slagstad and Støle-Hansen 1991; Koseff et al. 1993; Sharples and Tett 1994; Donaghay and Osborn 1997; Lucas et al. 1998). Our results will show that the earlier theoretical concepts developed by Riley et al. (1949), Sverdrup (1953), and Huisman et al. (1999*b*) can be integrated into a single unifying theory.

The Model

Light Gradient

We consider a water column with a cross section of one unit area. Let z denote the depth coordinate within the water column, where z runs from 0 at the top to a maximum depth, z_m, at the bottom. Let $I(z, t)$ denote the light intensity at depth z and time t, and let $\omega(z, t)$ denote the phytoplankton population density (cells per unit volume) at depth z and time t. Photons are absorbed by water, clay particles, phytoplankton, and many other light-absorbing substances. We assume that the light gradient follows Lambert-Beer's law, which states that the light intensity at depth z and time t is

$$I(z, t) = I_{in} \exp\left[-\int_0^z k\omega(\sigma, t)d\sigma - K_{bg}z\right]. \quad (1)$$

Here, I_{in} is the incident light intensity, k is the specific light attenuation coefficient of the phytoplankton, σ is an integration variable, and K_{bg} is the total background attenuation due to all nonphytoplankton components. We note that this formulation includes light absorption by phytoplankton. Thus, the light gradient changes with a change in the phytoplankton population density distribution.

Population Dynamics

The changes in phytoplankton population density can be described by a partial differential equation:

$$\frac{\partial \omega}{\partial t} = g(I)\omega - v\frac{\partial \omega}{\partial z} + D\frac{\partial^2 \omega}{\partial z^2}. \quad (2)$$

Here, $g(I)$ is the specific growth rate of phytoplankton as a function of the local light intensity I, v is the sinking velocity of the phytoplankton, and D is the turbulent-diffusion coefficient.

The specific growth rate in equation (2) depends on the balance between production and losses:

$$g(I) = p(I) - \ell, \quad (3)$$

where $p(I)$ is the specific production rate as an increasing function of light intensity, with $p(0) = 0$, and ℓ is the specific loss rate. In all our simulations, we used the following $p(I)$ function (Monod 1950; Huisman 1999):

$$p(I) = \frac{p_{max}I}{H + I}, \quad (4)$$

where p_{max} is the maximal specific production rate and H is a half-saturation constant. We emphasize, however, that the results presented in this article rely on the qualitative behavior of the $p(I)$ relation (i.e., $p(0) = 0$ and $dp/dI > 0$) rather than on its specific form.

Substituting equations (1) and (3) into equation (2) yields our key equation:

$$\frac{\partial \omega}{\partial t} = p\left(I_{in}e^{-\int_0^z k\omega(\sigma, t)d\sigma - K_{bg}z}\right)\omega - \ell\omega - v\frac{\partial \omega}{\partial z} + D\frac{\partial^2 \omega}{\partial z^2}. \quad (5)$$

The first term on the right-hand side indicates that the specific production rate at a certain depth depends on the light intensity at this depth, which in turn depends (via Lambert-Beer's Law) on all population densities above this depth. Owing to this integral term, equation (5) can be classified as an integro-partial differential equation.

We assume zero-flux boundary conditions:

$$v\omega(z, t) - D\frac{\partial \omega}{\partial z}(z, t) = 0, \quad \text{at } z = 0 \text{ and } z = z_m. \quad (6)$$

That is, there is no influx or efflux of phytoplankton, neither at the top nor at the bottom of the water column.

It is useful to keep track not only of the local population densities but also of the total phytoplankton population in the entire water column. This can be expressed as the total population size per unit surface area, W, defined by

Table 1: Parameters used in the simulations

Symbol	Meaning	Value	Units
Variables:			
I	Light intensity	…	μmol photons m^{-2} s^{-1}
ω	Population density	…	cells m^{-3}
W	Population size per unit surface area	…	cells m^{-2}
Parameters:			
D	Turbulent diffusion	1	cm^2 s^{-1}
H	Half-saturation constant of light-limited growth	30	μmol photons m^{-2} s^{-1}
I_{in}	Incident light intensity	350	μmol photons m^{-2} s^{-1}
K_{bg}	Background turbidity	.2	m^{-1}
k	Specific light attenuation of phytoplankton	15×10^{-12}	m^2 cell^{-1}
ℓ	Specific loss rate	.01	h^{-1}
p_{max}	Maximal specific production rate	.04	h^{-1}
v	Vertical velocity	.04	m h^{-1}
z_m	Water-column depth	20	m

$$W(t) = \int_0^{z_m} \omega(z, t)dz. \tag{7}$$

Using equation (2) and the boundary conditions, the population size per unit surface area changes with time according to

$$\frac{dW}{dt} = \int_0^{z_m} g(I(z, t))\omega(z, t)dz, \tag{8}$$

where the flux terms canceled because the boundaries are closed.

Numerical Simulations

The model predictions are analyzed using a combination of analytical and numerical techniques. Numerical simulation of integro-partial differential equations is quite challenging. Our simulations were based on a finite volume method, with spatial discretization of the spatial differential operators as well as the integral term. The diffusion term was discretized symmetrically, whereas a third-order upwind method was used for the advection term (e.g., Hirsch 1988). The resulting system of stiff ordinary differential equations (ODEs) was integrated over time using the implicit integration techniques of Brown et al. (1989). Our simulation techniques are explained in more detail in Huisman et al. (2001).

Parameter Values

We have attempted to parameterize the simulations as realistically as possible (table 1). Phytoplankton growth parameters were chosen within the typical ranges measured for freshwater phytoplankton species in the culture collection of the Laboratory of Aquatic Microbiology, University of Amsterdam, The Netherlands (e.g., Visser et al. 1996, 1997; De Nobel et al. 1998; Huisman 1999; Huisman et al. 1999a). Phytoplankton sinking velocities generally range from close to zero for small species like *Chlorella* to about $v = 0.1$ m h^{-1} for large phytoplankton species like *Stephanodiscus* (Smayda 1970; Reynolds 1984; Sommer 1984). The vertical turbulent-diffusion coefficient of lakes and oceans may vary over several orders of magnitude, from $D < 0.1$ cm^2 s^{-1} during quiescent periods to $D > 100$ cm^2 s^{-1} during periods of intense mixing (Denman and Gargett 1983; MacIntyre 1993). We used a background turbidity of $K_{bg} = 0.2$ m^{-1}, which is typical for clear lakes and clear coastal waters (Kirk 1994).

Conditions for Bloom Development

Phytoplankton Depth Profiles

According to our numerical simulations, the phytoplankton depth profile develops toward a stationary distribution. We shall indicate the stationary distribution by a superscript asterisk. What do the stationary depth profiles for sinking phytoplankton species look like?

One trivial solution for the stationary depth profile is, of course, that there are no phytoplankton at any depth at all. More precisely, $\omega^*(z) = 0$ for all z is, indeed, a stationary solution of equation (5). If the phytoplankton population develops toward this trivial solution, bloom

development is impossible. Hence, we say that there is "no bloom."

Alternatively, under suitable light conditions, the phytoplankton population may develop toward a positive stationary density distribution (i.e., $W^* > 0$). In this case, we say that there is "bloom development." Figure 1 shows a variety of stationary depth profiles obtained by numerical simulation, in which we gradually decreased the turbulent-diffusion coefficient. This illustrates that the stationary depth profile can have a local population-density maximum below the surface. Such a local population-density maximum develops if phytoplankton growth rates exceed both sinking rates and mixing rates. Interestingly, if turbulent diffusion is further decreased, below 0.1 cm^2 s^{-1}, the entire phytoplankton population sinks to the bottom of the water column and vanishes in the dark.

Bloom Development

What are the conditions favorable for bloom development of sinking phytoplankton species? In figure 2A, we plotted
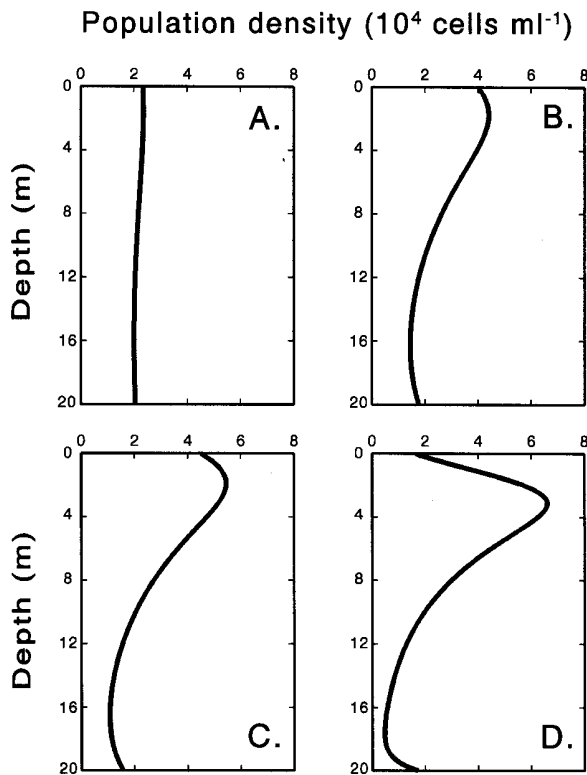
Population density (10^4 cells ml^{-1})

Figure 1: Stationary depth profiles of sinking phytoplankton for four different turbulence levels. Parameter values as in table 1, except (*A*) $D = 10$ cm^2 s^{-1}, (*B*) $D = 1$ cm^2 s^{-1}, (*C*) $D = 0.5$ cm^2 s^{-1}, and (*D*) $D = 0.1$ cm^2 s^{-1}.
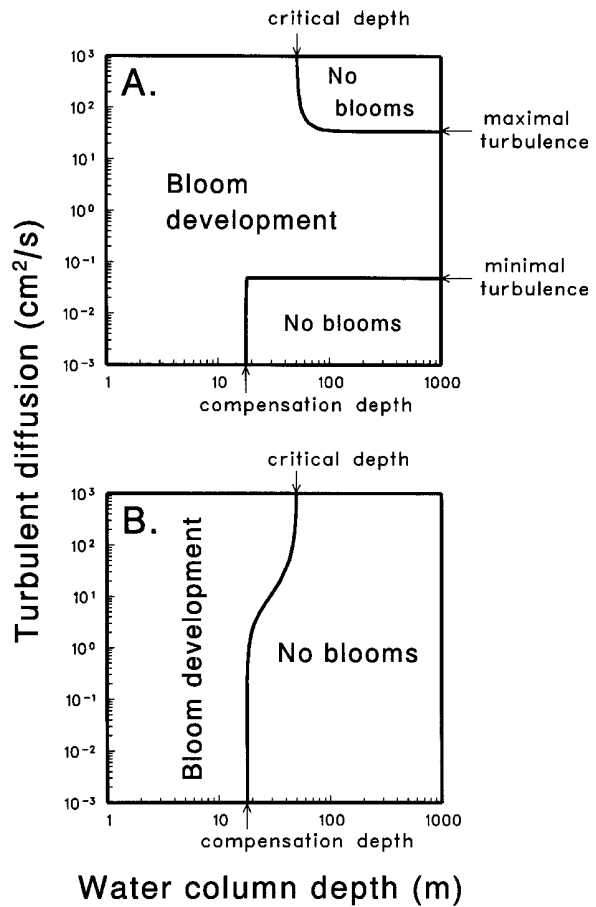

Water column depth (m)

Figure 2: Combinations of water-column depth, z_m, and turbulent-diffusion coefficient, D, that allow a phytoplankton bloom and combinations that prevent a phytoplankton bloom. *A*, Phytoplankton species with a moderate sinking velocity of $v = 0.04$ m h^{-1}. *B*, Phytoplankton species with a high sinking velocity of $v = 0.40$ m h^{-1}. The graphs are each based on a grid of $30 \times 60 = 1{,}800$ simulations. Parameter values as in table 1.

the regions of bloom development and regions of no blooms for a wide range of different water-column depths and turbulent diffusivities. Note the log scales of the axes: the graphs span the entire spectrum from shallow, quiescent lakes to deep, turbulent oceans. The left part of figure 2A considers shallow waters. In shallow waters, there is sufficient light for bloom development, irrespective of the phytoplankton distribution over depth. Hence, blooms can develop. The upper-right corner of figure 2A considers deep waters with a high turbulent mixing rate. Here, the phytoplankton population is mixed uniformly over great depths, and the average light conditions over the entire water column are insufficient for a net positive growth rate. Hence, blooms do not develop. The lower-right cor-

ner of figure 2*A* considers deep waters with a low turbulent mixing rate. Here, sinking rates exceed growth rates and mixing rates, and the phytoplankton population sinks downward to great depths. Consequently, blooms do not develop either. Most surprisingly, blooms of sinking species can develop in deep systems with intermediate mixing rates (middle right of fig. 2*A*). In this parameter region, growth rates exceed mixing rates so that uniform mixing over the entire depth of the water column is prevented. Moreover, turbulent mixing rates exceed sinking rates so that large downward fluxes of phytoplankton are avoided. As a consequence, sinking species can maintain a population in the euphotic zone at intermediate mixing rates.

Interestingly, the no-bloom areas in figure 2*A* are bound by nearly horizontal and vertical lines. This implies that the effects of water-column depth and turbulent diffusion on phytoplankton-bloom development are essentially independent of one another. Hence, we can recognize a "critical depth," a "compensation depth," a "maximal turbulence," and a "minimal turbulence" (fig. 2*A*). We call the region between the maximal and minimal turbulence the "turbulence window" for sinking phytoplankton.

Figure 3 plots the total population size per unit surface area, *W*, as a function of water-column depth and turbulent diffusion. The two no-bloom regions at low and high turbulence are clearly visible (cf. fig. 3 with fig. 2*A*). If the water column is shallow ($z_m < 10$ m), population size per unit surface area is a decreasing function of water-column depth, whereas it is independent of turbulence. Conversely, if the water column is deep ($z_m > 50$ m), population size per unit surface area is a unimodal function of turbulence, whereas it is independent of water-column depth. The two patterns are perpendicular to each other. This provides another illustration of the phase transition documented in this article; water-column depth determines the population size of phytoplankton in shallow systems, whereas turbulence determines the population size of phytoplankton in deep systems.

Explicit Expressions

It would be convenient, for both practical applications and a better general understanding, to have a fast method available to calculate the four critical parameters of figure 2*A*. We developed two procedures. First, we derived a fast and accurate algorithm, described in the appendix. Second, we derived analytical expressions for the four critical parameters, which are discussed below.

Critical Depth

The critical depth in figure 2 is equivalent to Sverdrup's (1953) concept of a critical depth. Intuitively, the idea is
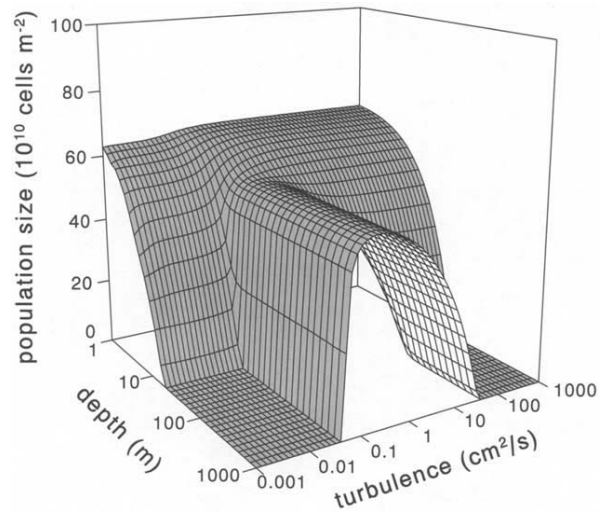

Figure 3: Population size per unit surface area, *W*, as a function of water-column depth and turbulent-diffusion coefficient. The graph is based on a grid of $30 \times 60 = 1,800$ simulations. Parameter values as in table 1.

that, in turbulent waters, phytoplankton are uniformly mixed throughout the water column (as in fig. 1*A*). As a result, the phytoplankton population has high production rates in the upper part of the water column but suffers losses throughout the water column. Hence, depth-integrated production rates will be less than depth-integrated loss rates if the water column becomes too deep. That is, bloom development in turbulent waters is impossible if water-column depth exceeds a critical depth.

Theory and experiments show that Sverdrup's critical depth can be reinterpreted in terms of a critical light intensity (Huisman and Weissing 1994; Huisman 1999; Huisman et al. 1999*b*). Accordingly, the critical depth, z_{cr}, can be written as

$$z_{cr} = \frac{\ln(I_{in}) - \ln(I_{out}^*)}{K_{bg}}, \qquad (9)$$

where I_{out}^* is the critical light intensity sensu Huisman and Weissing (1994).

Compensation Depth

The compensation depth, z_C, in figure 2 is the depth at which the compensation light intensity would be reached in the absence of phytoplankton. That is,

$$z_C = \frac{\ln(I_{in}) - \ln(I_C)}{K_{bg}}. \qquad (10)$$

Here, I_C is the compensation light intensity, defined as the light intensity at which specific production rate equals specific loss rate. That is, the compensation light intensity is defined by $g(I_C) = 0$. Intuitively, the idea is that, in systems with a low turbulence, the total phytoplankton population sinks to the bottom of the water column and growth conditions thus depend only on the light conditions at the bottom. A phytoplankton population located at the bottom of the water column cannot develop if light conditions at the bottom are less than the compensation light intensity. Thus, bloom development in quiet waters is impossible if water-column depth exceeds the compensation depth. We note that the critical depth is always deeper than the compensation depth (i.e., the critical light intensity is lower than the compensation light intensity; Huisman and Weissing 1994).

Maximal Turbulence

The maximal turbulence in figure 2*A* is equivalent to the critical turbulence described by Huisman et al. (1999*b*). The idea that underlies the concept of a maximal turbulence is that, if turbulent diffusion is less than a certain threshold value, phytoplankton populations may outgrow the turbulent mixing rate and may thus maintain a bloom in the upper well-lit part of the water column. Generally speaking, there is no simple analytical equation for the maximal turbulence. In the special case that the specific production rate is of the form $p(I) = aI^\alpha$, with $0 < \alpha \le 1$, we were able to derive an approximation for the maximal turbulence based on so-called Bessel functions approached by asymptotic expansion techniques. The derivation is involved and will be given elsewhere (Ebert et al. 2001). We remark that the linear case $p(I) = aI$ is included in the above derivation. For nonlinear $p(I)$ functions with saturating properties, such as equation (4), we recommend calculating the maximal turbulence by the algorithm outlined in the appendix.

Minimal Turbulence

The idea of a minimal turbulence is that, if turbulent diffusion becomes too low, there is no force that prevents sinking of the entire phytoplankton population. Hence, if turbulence is too low and the water column is deep, the entire phytoplankton population vanishes in the dark. Riley et al. (1949) showed that an exact equation for the minimal turbulence can be derived under the following simplifying assumptions: first, the vertical nature of the light gradient is neglected (i.e., $g(I) = g(I_{in})$ throughout the water column), but, second, the phytoplankton population vanishes at the bottom of the water column. These simplifications reduce equation (5) to a linear homogeneous partial differential equation with constant coefficients

$$\frac{\partial \omega}{\partial t} = g(I_{in})\omega - v\frac{\partial \omega}{\partial z} + D\frac{\partial^2 \omega}{\partial z^2}, \tag{11}$$

and boundary conditions

$$v\omega(0, t) - D\frac{\partial \omega}{\partial z}(0, t) = 0 \text{ and } \omega(z_m, t) = 0. \tag{12}$$

Under these simplifying assumptions, one can derive that the minimal turbulence required for population persistence in deep systems is (Riley et al. 1949)

$$D_{min} = \frac{v^2}{4g(I_{in})}. \tag{13}$$

A derivation of the same equation was recently presented by Speirs and Gurney (2001) in the context of species inhabiting rivers subjected to downstream drift. Shigesada and Okubo (1981) showed that equation (13) still holds if self-shading of the phytoplankton population is included but the background turbidity of the water column is neglected.

Since the derivation of equation (13) neglects the vertical light gradient generated by the background turbidity of the water column, this equation is at best an approximation of the minimal turbulence predicted by our full model. More precisely, numerical simulations indicate that equation (13) is an accurate approximation of the minimal turbulence in waters with a low background turbidity, whereas minimal turbulence is somewhat higher than predicted by equation (13) in waters with a high background turbidity (fig. 4). We thus recommend equation (13) to calculate the minimal turbulence in oceanic waters and clear lakes, whereas the algorithm outlined in the appendix is recommended for more turbid ecosystems.

Effects of Sinking Velocity

We note, from equations (9) and (10), that the critical depth and compensation depth are both independent of the sinking velocity of the phytoplankton. In contrast, according to equation (13), the minimal turbulence increases with the square of phytoplankton sinking velocity. Moreover, numerical simulations indicate that the maximal turbulence decreases with sinking velocity. Therefore, if the phytoplankton sinking velocity is too high, the minimal turbulence and maximal turbulence merge and disappear. Thus, while phytoplankton species with a moderate sinking speed can persist in deep waters (fig. 2*A*), phytoplank-
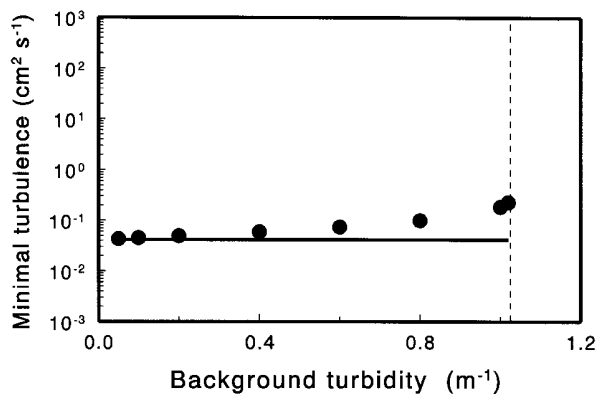
Figure 4: Minimal turbulence as a function of background turbidity, predicted by the full model (*dots*) and predicted by equation (13) (*solid line*). Phytoplankton blooms cannot be sustained if background turbidity exceeds the vertical dashed line. Parameter values as in table 1.

ton species with a high sinking speed cannot persist in deep waters (fig. 2*B*).

Discussion

It is not difficult to understand how sinking phytoplankton species can maintain populations in optically shallow waters. In such waters, phytoplankton populations may sink to the bottom sediment, but light conditions near the bottom sediment may still be sufficient to sustain these populations (fig. 2). Obviously, our model simplification that phytoplankton cannot leave the system at the bottom sediment may not hold for all aquatic ecosystems. For instance, the model might be extended by introducing boundary conditions that mimic burial of phytoplankton in the sediment or grazing on phytoplankton by benthic filter feeders (e.g., Koseff et al. 1993). Such additional losses at the bottom sediment will make it harder for sinking phytoplankton to persist. Apart from these additional complications, however, light conditions themselves are generally sufficient for the persistence of sinking phytoplankton populations in optically shallow waters.

The question here is how sinking phytoplankton species can persist in optically deep waters, like the oceans, as well. The key finding in this article is the existence of a "turbulence window" that allows persistence of sinking phytoplankton populations in deep waters (figs. 2*A*, 3). If turbulence levels are less than a minimal turbulence, sinking rates dominate over growth rates and mixing rates. In this case, the phytoplankton population sinks downward and is lost from the euphotic zone. If turbulence levels exceed a maximal turbulence, vertical mixing rates dominate over growth and sinking. In this case, the phyto-

plankton population is uniformly mixed and receives insufficient light in the deeper parts of the water column to persist. At intermediate turbulence levels, however, growth rates in the euphotic zone may exceed both sinking losses and mixing rates. Under these circumstances, a population of sinking phytoplankton may develop in the upper part of the water column. Thus, at intermediate turbulence levels, sinking phytoplankton species are capable of maintaining a population within the euphotic zone.

Our results indicate that arguments of previous authors (e.g., Hutchinson 1967), that there must be a strong selection pressure against sinking phytoplankton species, need not hold. At least, these arguments need not hold for deep waters whose characteristics fall within the turbulence window since deep waters located within the turbulence window can sustain sinking phytoplankton. The turbulence window will disappear, however, if the phytoplankton sinking velocity is pushed beyond a certain threshold value (fig. 2*B*). Thus, in line with intuitive reasoning, sinking phytoplankton cannot persist in deep waters if their sinking speed is too high; only phytoplankton with low to moderate sinking velocities can be sustained.

Does the theory match reality? We have attempted to choose our parameter values to be as realistic as possible. This revealed that the turbulence window should disappear at a phytoplankton sinking velocity of about $v \approx 0.4$ m h^{-1} (fig. 2*B*). It is intriguing that the highest sinking velocities of living phytoplankton cells, of large oceanic diatoms of the *Coscinodiscus* genus and the giant *Ethmodiscus rex*, are indeed approximately 0.3–0.6 m h^{-1} (Smayda 1970). Also, the theory predicts that phytoplankton species with such high sinking speeds should be restricted to waters with a narrow window of vertical turbulent diffusivities, somewhere in the range of 1–10 cm^2 s^{-1}. This range is not unrealistic at all (Denman and Gargett 1983). Hence, even quantitatively, there is a good correspondence between the model predictions and reality.

In conclusion, it is interesting to compare our findings with the earlier theoretical concepts developed by Riley et al. (1949), Sverdrup (1953), and Huisman et al. (1999*b*). This article shows that these concepts are neither overlapping nor mutually exclusive. Instead, these earlier concepts form different elements in one coherent theory. The critical depth in our figures is equivalent to Sverdrup's critical depth (Sverdrup 1953; Platt et al. 1991). The minimal turbulence in our figures corresponds to the classic relation, in equation (13), derived by Riley et al. (1949) and Shigesada and Okubo (1981). The maximal turbulence in our figures is equivalent to the critical turbulence found by Huisman et al. (1999*b*, 1999*c*). We have thus shown that the different concepts developed by these earlier authors can be integrated into a single unifying theory.

APPENDIX

A Fast Algorithm

To estimate the critical depths and critical turbulences, one could run the integro-partial differential equation (integro-PDE) until steady state for a couple of thousand times in a fine grid of z_m values and D values. However, this is a time-consuming procedure that requires quite a number of programming skills. As an alternative, this appendix develops a simple algorithm to calculate the critical depths and critical turbulences. The algorithm is fast, accurate, and very easy to apply. The trick is twofold: first, on the boundary lines between the bloom and the no-bloom region (fig. 2), the integro-PDE can be reduced to a system of two ordinary differential equations (ODEs), and second, the boundary-value problem of this ODE system can be translated into an initial-value problem.

Development of the Method

We consider the transition from the bloom to the no-bloom region. At this transition, the phytoplankton population density is negligibly small. More precisely, at this transition and also in the no-bloom area itself, we have

$$\int_0^z k\omega^*(\sigma)d\sigma \ll K_{bg}z.$$

Hence, the light intensity I can be approximated by $I_{in}\exp(-K_{bg}z)$. This implies that the equation defining the stationary population density distribution reduces to a second-order ODE without an integro-term:

$$g(I_{in}e^{-K_{bg}z})\omega^* - v\frac{d\omega^*}{dz} + D\frac{d^2\omega^*}{dz^2} = 0. \qquad (A1)$$

This equation can be rewritten as a system of two coupled first-order ODEs:

$$\frac{d\omega^*}{dz} = \psi^*,$$

$$\frac{d\psi^*}{dz} = -\frac{1}{D}g(I_{in}e^{-K_{bg}z})\omega^* + \frac{v}{D}\psi^*, \qquad (A2)$$

with boundary conditions, from equation (6),

$$v\omega^*(0) - D\psi^*(0) = 0 \text{ and } v\omega^*(z_m) - D\psi^*(z_m) = 0. \qquad (A3)$$

Equations (A2) and (A3) are linear and homogeneous in ω^* and ψ^*. Hence, if there exists a solution $\omega^*(z)$, then there also exists a solution $c\omega^*(z)$ for any arbitrary c. The free initial condition $\omega^*(0)$ is therefore arbitrary, and we may just as well work with $\omega^*(0) = 1$. Therefore, using the first boundary condition in equations (A3), the initial values for the two ODEs in equations (A2) can be defined as

$$\omega^*(0) = 1 \text{ and } \psi^*(0) = \frac{v}{D}. \qquad (A4)$$

The boundary-value problem has thus been transformed into an initial-value problem. Accordingly, we obtain the following numerical recipe.

Numerical Recipe

Choose a value for the turbulent-diffusion coefficient D. Starting from the initial conditions given in equations (A4), the two coupled ODEs in equations (A2) can be integrated forward in z until the solution hits on either $v\omega^*(z) - D\psi^*(z) = 0$ or $\omega^*(z) = 0$.

If we find $v\omega^*(z) - D\psi^*(z) = 0$ at some depth z, then the second boundary condition in equations (A3) is satisfied. Hence, this depth z is either the critical depth or the compensation depth.

Alternatively, if we find $\omega^*(z) = 0$ at some depth z, then the second boundary condition in equations (A3) cannot be satisfied with positive $\omega^*(z)$. In this case, the critical depth and compensation depth do not exist. That is, we have used a value of D somewhere in the parameter region between the minimal turbulence and maximal turbulence.

Repeat this procedure for various values of D, and plot the critical depth or compensation depth whenever they exist. This yields the graphs in figure 2.

As a check, we compared the predictions of this algorithm against the stationary results obtained by numerical simulation of the full integro-PDE. Both methods always yielded the same critical depths, the same compensation depths, and the same critical turbulences, but the algo-

rithm is several orders of magnitude faster than numerical simulation of the full integro-PDE.

We emphasize that if one is interested in the time development of the population density distribution as well, then one should resort to simulation of the full model. The fast algorithm outlined in this appendix calculates only the values of the critical depths and critical turbulences (fig. 2).

Literature Cited

Arrigo, K. R., D. H. Robinson, D. L. Worthen, R. B. Dunbar, G. R. DiTullio, M. VanWoert, and M. P. Lizotte. 1999. Phytoplankton community structure and the drawdown of nutrients and CO_2 in the Southern Ocean. Science (Washington, D.C.) 283:365–367.

Brown, P. N., G. D. Byrne, and A. C. Hindmarsh. 1989. VODE: a variable-coefficient ODE solver. SIAM (Society for Industrial and Applied Mathematics) Journal on Scientific and Statistical Computing 10:1038–1051.

Denman, K. L., and A. E. Gargett. 1983. Time and space scales of vertical mixing and advection of phytoplankton in the upper ocean. Limnology and Oceanography 28:801–815.

De Nobel, W. T., H. C. P. Matthijs, E. von Elert, and L. R. Mur. 1998. Comparison of the light-limited growth of the nitrogen-fixing cyanobacteria *Anabaena* and *Aphanizomenon.* New Phytologist 138:579–587.

DiTullio, G. R., J. M. Grebmeier, K. R. Arrigo, M. P. Lizotte, D. H. Robinson, A. Leventer, J. P. Barry, M. L. VanWoert, and R. B. Dunbar. 2000. Rapid and early export of *Phaeocystis antarctica* blooms in the Ross Sea, Antarctica. Nature 404:595–598.

Donaghay, P. L., and T. R. Osborn. 1997. Toward a theory of biological-physical control of harmful algal bloom dynamics and impacts. Limnology and Oceanography 42:1283–1296.

Ebert, U., M. Arrayás, N. Temme, B. Sommeijer, and J. Huisman. 2001. Critical conditions for phytoplankton blooms. Bulletin of Mathematical Biology 63:1095–1124.

Falkowski, P. G., R. T. Barber, and V. Smetacek. 1998. Biogeochemical controls and feedbacks on ocean primary production. Science (Washington, D.C.) 281:200–206.

Hirsch, C. 1988. Numerical computation of internal and external flows. I. Fundamentals of numerical discretization. Wiley, Chichester.

Huisman, J. 1999. Population dynamics of light-limited phytoplankton: microcosm experiments. Ecology 80:202–210.

Huisman, J., and F. J. Weissing. 1994. Light-limited growth and competition for light in well-mixed aquatic environments: an elementary model. Ecology 75:507–520.

Huisman, J., R. R. Jonker, C. Zonneveld, and F. J. Weissing. 1999*a.* Competition for light between phytoplankton species: experimental tests of mechanistic theory. Ecology 80:211–222.

Huisman, J., P. van Oostveen, and F. J. Weissing. 1999*b.* Critical depth and critical turbulence: two different mechanisms for the development of phytoplankton blooms. Limnology and Oceanography 44:1781–1788.

———. 1999*c.* Species dynamics in phytoplankton blooms: incomplete mixing and competition for light. American Naturalist 154:46–68.

Huisman, J., M. Arrayás, U. Ebert, and B. Sommeijer. 2001. Sinking phytoplankton species. Report MAS-R0105, National Research Center for Mathematics and Computer Science, Amsterdam.

Hutchinson, G. E. 1967. A treatise on limnology. II. Introduction to lake biology and the limnoplankton. Wiley, New York.

Jamart, B. M., D. F. Winter, K. Banse, G. C. Anderson, and R. K. Lam. 1977. A theoretical study of phytoplankton growth and nutrient distribution in the Pacific Ocean off the northwest U.S. coast. Deep-Sea Research 24:753–773.

Kirk, J. T. O. 1994. Light and photosynthesis in aquatic ecosystems. 2d ed. Cambridge University Press, Cambridge.

Koseff, J. R., J. K. Holen, S. G. Monismith, and J. E. Cloern. 1993. Coupled effects of vertical mixing and benthic grazing on phytoplankton populations in shallow, turbid estuaries. Journal of Marine Research 51:843–868.

Lucas, L. V., J. E. Cloern, J. R. Koseff, S. G. Monismith, and J. K. Thompson. 1998. Does the Sverdrup critical depth model explain bloom dynamics in estuaries? Journal of Marine Research 56:375–415.

MacIntyre, S. 1993. Vertical mixing in a shallow, eutrophic lake: possible consequences for the light climate of phytoplankton. Limnology and Oceanography 38:798–817.

Mann, K. H., and J. R. N. Lazier. 1996. Dynamics of marine ecosystems: biological-physical interactions in the oceans. 2d ed. Blackwell, Oxford.

Monod, J. 1950. La technique de culture continue, théorie et applications. Annales de l'Institut Pasteur (Paris) 79:390–410.

Platt, T., D. F. Bird, and S. Sathyendranath. 1991. Critical depth and marine primary production. Proceedings of the Royal Society of London B, Biological Sciences 246:205–217.

Reynolds, C. S. 1984. The ecology of freshwater phytoplankton. Cambridge University Press, Cambridge.

Riley, G. A., H. Stommel, and D. F. Bumpus. 1949. Quantitative ecology of the plankton of the western North

Atlantic. Bulletin of the Bingham Oceanographic Collection Yale University 12:1–169.

Sharples, J., and P. Tett. 1994. Modelling the effect of physical variability on the midwater chlorophyll maximum. Journal of Marine Research 52:219–238.

Shigesada, N., and A. Okubo. 1981. Analysis of the self-shading effect on algal vertical distribution in natural waters. Journal of Mathematical Biology 12:311–326.

Slagstad, D., and K. Støle-Hansen. 1991. Dynamics of plankton growth in the Barents Sea: model studies. Polar Research 10:173–186.

Smayda, T. J. 1970. The suspension and sinking of phytoplankton in the sea. Oceanography and Marine Biology an Annual Review 8:353–414.

Sommer, U. 1984. Sedimentation of principal phytoplankton species in Lake Constance. Journal of Plankton Research 6:1–14.

Speirs, D. C., and W. S. C. Gurney. 2001. Population persistence in rivers and estuaries. Ecology 82:1219–1237.

Sverdrup, H. U. 1953. On conditions for the vernal blooming of phytoplankton. Journal du Conseil Conseil Permanent International pour l'Exploration de la Mer 18:287–295.

Visser, P. M., L. Massaut, J. Huisman, and L. R. Mur. 1996. Sedimentation losses of *Scenedesmus* in relation to mixing depth. Archiv für Hydrobiologie 136:289–308.

Visser, P. M., J. Passarge, and L. R. Mur. 1997. Modelling vertical migration of the cyanobacterium *Microcystis*. Hydrobiologia 349:99–109.